

BI-DIMENSIONAL RECONSTRUCTION OF A BUNSEN BURNER FLAME

Anton Skyrda Veríssimo

Instituto Nacional de Pesquisas Espaciais, Rodovia Presidente Dutra km 40, Cachoeira Paulista – SP, Brazil
e-mail antonskyrda@yahoo.com.br

Pedro Teixeira Lacava

Instituto Tecnológico de Aeronáutica, Praça Marechal Eduardo Gomes 50, São José dos Campos – SP, Brazil
placava@ita.br

Antônio Osny de Toledo

Instituto de Estudos Avançados, Rodovia dos Tamoios Km 5,5, São José dos Campos – SP, Brazil
osny@ieav.cta.br

Abstract. *Using non-intrusive techniques to study physical and chemical properties of flames take to more realistic results. The tomographic backprojection algorithm together with the Algebraic Reconstruction Technique (ART), can reconstruct an object internal structure or properties of a restrict region of the space from their projection data. This work presents a few data tomography technique using the emission of light by a Bunsen burner laminar flame . The chemicals radicals in a flame emit light in a series of characteristics wavelength. With some CCD cameras and light filters one can mount a simple tomograph to obtain the bidimensional radicals distribution in a flame cross section through computerized tomography techniques (CT).*

Keywords: *computerized tomography technique, image reconstruction, flame diagnostics, Bunsen burner flame.*

1. Introduction

The problem of image reconstruction from projections has arisen independently in a large number of scientific fields. An important version of the problem in combustion is that of obtaining the products of combustion density distribution within the flame from multiple light emission projections. This process is referred to as *emission computerized tomography*.

The computerized tomography, CT, is a reconstruction technique from projections that reproduces the picture from the projection data of the picture.

The quantum transitions of radicals, in flames, produce electromagnetic waves emission, i.e. light, that carry information about the phenomena from the flame physical region, called reconstruction region, RR. A number of arrays of detectors are placed around the flame with all their optical axes in the same plane containing the RR, which in this case, is a thin slice. In the physical model worked here, each detector 'sees' the sum of the light produced in a frontal line, Fig. 1a. At the same time all the arrays of detectors are triggered, and each array scans an angular image of the flame to be studied, Fig. 1b.

The light from each chemical radical due to quantum decays, presents a characteristic discrete spectra, from ultra-violet (UV) to infra-red (IR), depending on the temperature. In this way, one can scan a selected radical emission choosing an optical filter that selects the proper wavelength.

In this work it was used one CCD camera (an array of detectors behind an optical system) supported by a mechanical arm which could move it around the RR, Fig. 1b.

After the acquisition, the image is transferred to file in a computer, and the data are treated by a computational algorithm and graphic software to produce the final result, i.e., the image.

In medical applications, the number of measured lines is usually huge ($10^5 - 10^6$ in each slice) with a very good resolution. However, in many applications of tomography to problems of science and engineering, the number of data is much smaller, say 20 to 200. For such small data sets the very notation of resolution becomes questionable, this is the Few Data CT.

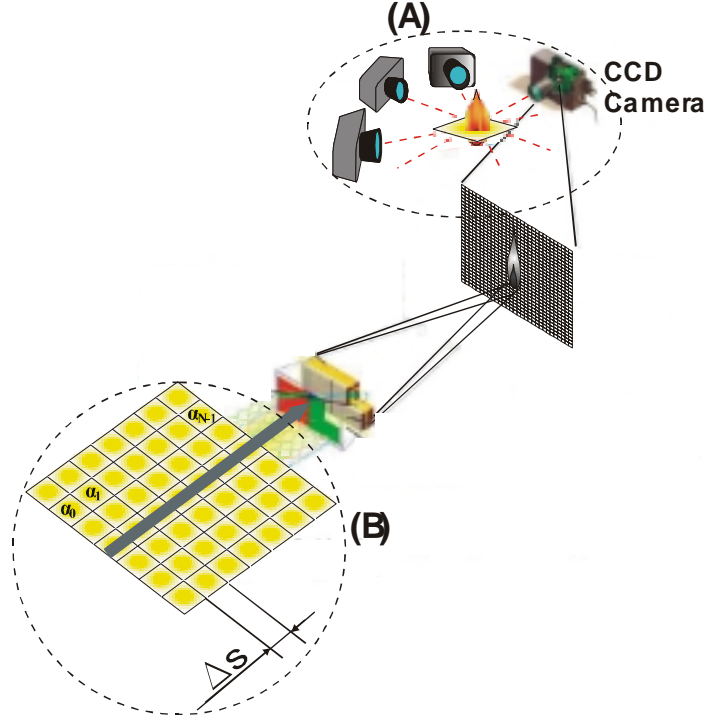


Figure 1. TC data acquisition through a RR; a) Angular CCD's cameras positions around the RR; emerging with intensity, I . The α_i 's are the extinction (absorption plus scattering) linear coefficient of each layer, and L is the integration line. b) A light beam is formed within the RR.

Each photon produced in the pixels of the RR aligned with and driven to a specific detector of the array is summed up. So this give rise to a line integral, of the light in that line, that could be expressed like a Radon Transform of the light production function. In this first approach one not consider the absorption and refraction of the light from the physical region of the flame.

2. The Mathematical Approach

The common mathematical basis whose these algorithms come from are the Radon and Abel transforms with their respective inverses (Radon, 1917), and the expansion reconstruction methods by finite series (Gordon and Hermann, 1970) or Algebraic Reconstruction Technique, ART. In this work the ART is applied.

Mathematically, first of all, one defines a picture function, f , of two variables whose value is zero outside the picture region, which can be a square, for example, Fig. 1a. The Radon transform, \mathfrak{R} , of f is defined for real numbers pairs (l, θ) , as follows:

$$[\mathfrak{R} f](l, \theta) = \int_{-\infty}^{\infty} f\left(\sqrt{l^2 + z^2}, \theta + \tan^{-1}\left(\frac{z}{l}\right)\right) dz \quad \text{if } l \neq 0 \quad (1)$$

$$[\mathfrak{R} f](0, \theta) = \int_{-\infty}^{\infty} f\left(z, \theta + \frac{\pi}{2}\right) dz \quad (2)$$

where the parameters are taken from the coordinate system shown in the Fig. 2 and z is a coordinate along the L line.

f is a function integrated over the L line in the Radon transform and is exactly the parameter to be known. Generally, one has this integral results and one intends to obtain the function f :

$$[\mathfrak{R}^{-1} \mathfrak{R} f](r, \phi) = f(r, \phi) \quad (3)$$

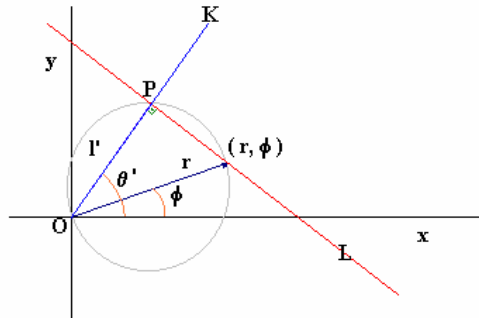


Figure 2. Relationship between the (r, ϕ) space and the (l, θ) space. In the (r, ϕ) space K is a half line through the origin O making an θ' angle with the baseline over x -axes. The point (r, ϕ) is considered given and L is the line through (r, ϕ) perpendicular to K . L meets K at P which is at the distance l' from O .

This operation is done by the Radon inverse transform, \mathfrak{R}^{-1} . In order to understand the inverse Radon operator, one expresses it as sequence of simpler operators:

$$\mathfrak{R}^{-1} = -\frac{1}{2\pi} B H_Y D_Y \quad (4)$$

where D_Y is a partial differential operator, H_Y is the Hilbert transform operator, and B is the back projection operator.

The simplest algorithm for reconstruction is that one to estimate the density at a point (pixel) by adding all the ray sums of the rays through that point. This is called the *backprojection method*. Note that the traditional tomography is essentially a backprojection method that, in general, does not produces good images as the more sophisticated techniques.

For implementation of the inverse Radon transform on a computer one have to replace these continuous operators by discrete ones which operates on functions with a finite numbers of arguments. This is done at the very end of the derivation of the reconstruction algorithm. In the series expansion approach, the problem itself is discretized at the very beginning: estimating the function is translated into finding a finite series of numbers. It is assumed that one fix a set of basis picture, whose linear combination gives adequate approximation to any picture f one wishes to reconstruct.

Such approach is done by digitization of the function picture by dividing the picture into small regions called pixels, given the equation

$$f(r, \phi) = \sum_{j=1}^J x_j b_j(r, \phi) \quad (5)$$

where, J is the number of pixels, x_j is the average value of f inside the j th pixel or the image vector components, and $b_j(r, \phi)$ is the basis pictures.

In order to show how the image reconstruction problems translates into a discrete problem using series expansion approach one can sees that

$$\mathfrak{R}_i f = \sum_{j=1}^J x_j \mathfrak{R}_i b_j \quad (6)$$

For $r_{ij} = \mathfrak{R}_i b_j$, one has

$$y = R x \quad (7)$$

In this way, the reconstruction problems, based in Eq.(7), leads to the following discrete reconstruction problem:
Give On the data y , estimate the image vector x .

What is ART? All series expansion methods are procedures for the solution of the discrete reconstruction problem. As it has been briefly said above this is the problem of estimating an image vector x such that $y = Rx$, given a measurement vector y . All ART methods of image reconstruction are iterative procedures.

Considering a RR divided into $n \times n = n^2 = J$ pixels, the k th iterative step in ART can be described by a function μ_k , whose arguments are two J -dimensional vectors and one real number and whose value is a J -dimensional vector, $\mu_k : R^J \times R^J \times R \rightarrow R^J$ in mathematical language, and where R denotes the set of real numbers. The $(k+1)$ th iteration, in this method, can be written

$$x^{(k+1)} = \mu_k(x^{(k)}, r_{ik}, y_{ik}) \quad (8)$$

In words, a particular algebraic reconstruction technique is defined by a sequence of functions $\mu_0, \mu_1, \mu_2 \dots$. In order to get the $(k+1)$ st iterate one applies μ_k to the k th iterate, the i_k th row of the projection matrix R , and the i_k th component of the measurement vector y . Various ART methods differ from each other in the way the sequence of μ_k 's is chosen.

One way of choosing the μ_k 's is the following: for any J -dimensional vectors x and t and for any real number z ,

$$\mu_k(x, t, z) = \begin{cases} x + \frac{z - \langle t, x \rangle}{\langle t, t \rangle} t & \rightarrow \langle t, t \rangle \neq 0 \\ x & \rightarrow \langle t, t \rangle = 0 \end{cases} \quad (9)$$

where \langle , \rangle denotes the inner product of two J -dimensional vectors.

2.1 Numerical Approach

The Fig. 3 shows the image discretization into small elements of picture called pixels. The ray sum and the each pixel has the same width.

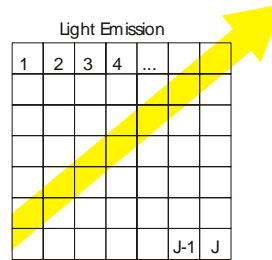


Figure 3. RR divided into J pixels showing the ray sum (Light Emission).

According to the Eq.6, the i -th ray sum is given by

$$\sum_{j=1}^J r_{ij} x_j \cong y_i \quad i=1, 2, \dots, M \quad (10)$$

where M is the number of ray sums in a particular angular projection.

The numerical approach used here is based on the Kaczmarz technique (Kaczmarz, 1937) and (Kak and Slaney, 1988).

$\vec{x} \in R^n$ is an arbitrary vector, where $n = \sqrt{J}$, whose components are the average emission of each pixel in the data acquisition moment. In practical application, the Eq.9 can be posed like:

$$nTC_i = N_i + \frac{S_p - R_p}{nP} \quad (11)$$

where nTC_i is the average emission in the i th pixel, N_i is the ray sum result in the i th pixel, S_p is the ray sum in that projection, R_p is the original projected ray sum, and nP is the number of pixels crossed by the ray sum.

In the iterative procedure the Eq. (11) is repeated until some convergence established by the user is reached.

3. The Experimental Set Up

To realize the experiment, a simple CT tomograph was mounted. A mechanical articulated arm, a CCD camera, and a goniometric table, Fig. 4, form it.

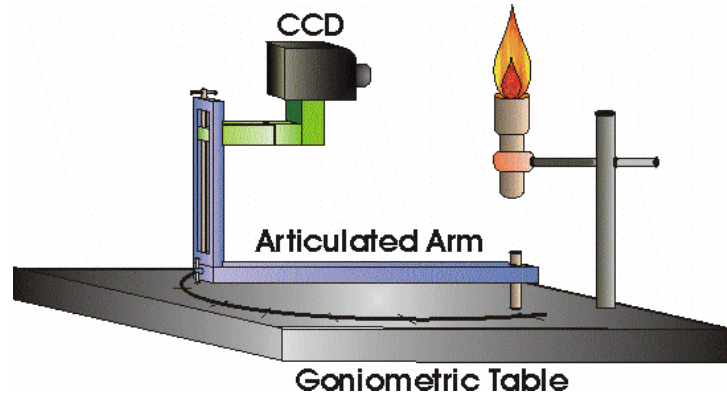


Figure 4. Simple tomograph sketch showing the Articulated Arm supporting the CCD camera over the Goniometric Table.

The mechanical articulated arm was made to support the CCD camera and to allow its horizontal, vertical, and radial freedom of motion, plus the rotation around a vertical axis. These rotational motions allow picturing the flame from several angular positions, and from the same distance.



Figure 5. The experimental setup.

The arm is supported by a table with angular graduation to locate it at different angles to picture the flame.

The camera is a CCD Marshall V-1070-EIA, with 480 vertical lines and 520 horizontal lines, with 0.02 lux of minimal sensibility. The CCD sensor dimensions are 7.95 mm by 6.45 mm, with exposition time between 1/125 and 1/10000 s. Were used Marshall objectives with optical filters in 515.14 nm, 65.99% transmittance, and 801 nm, 56.77% transmittance, corresponding to the quimiluminescent emission of the C_2 radical, and of soot, respectively.

The images were acquired through a Matrox Meteor/RGB electronic plate in a Pentium 133 MHz computer, 32 Mb ram memory, and saved in bitmap files. These files were treated and the images reconstructed with the MathCad™ software. A Bunsen burner, Fig. 5, with in a steady state flow, 0.1 g/s, produced the reconstruction object, a laminar flame 38 mm height.

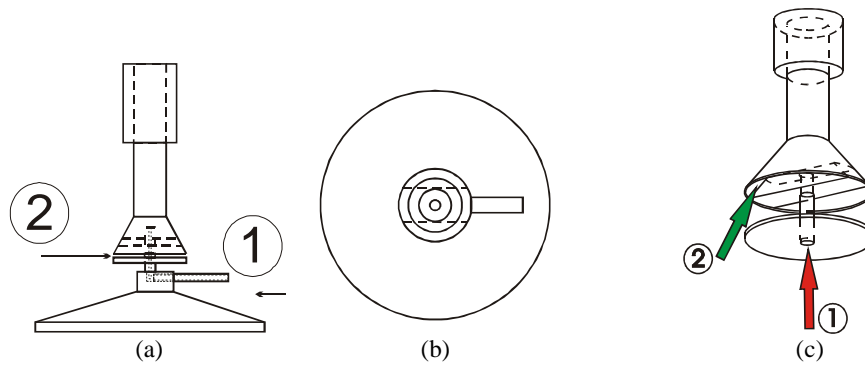


Figure 6. Bunsen burner geometry. a) Lateral sight (1) fuel injection (2) inflow air; b) Top sight and (c) tri-dimensional sight.

5.Results

The data acquisition was made at 0° , 30° , 60° , 90° , 120° . These data were monochromatic images, and, at each position, two filtered photos were taken (at 515.14 nm – C_2 radical and 801 nm - soot) from a 700 mm radial distance of the flame. Each filtered photo was an average over 50 photos.



Figure 7. The Bunsen burner flame photo.



a)



b)

Figure 8. Filtered photos: a) 801 nm , and b) 515.14 nm .

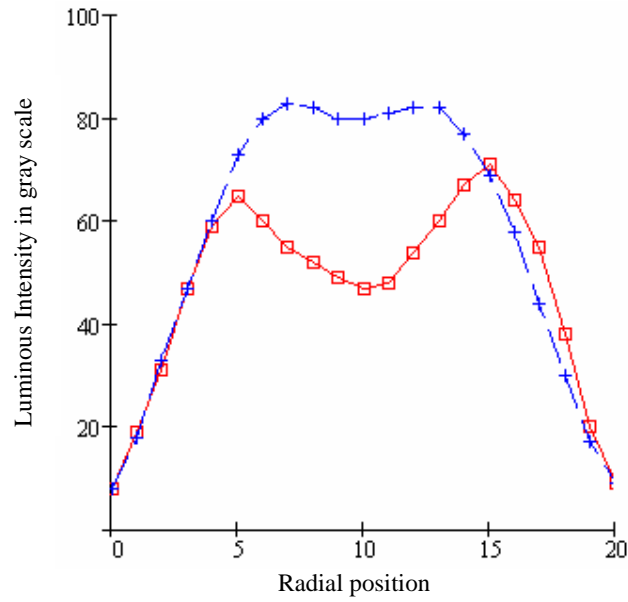


Figure 9. C₂ radical distribution (box, □), and soot (cross, +) at 0°.

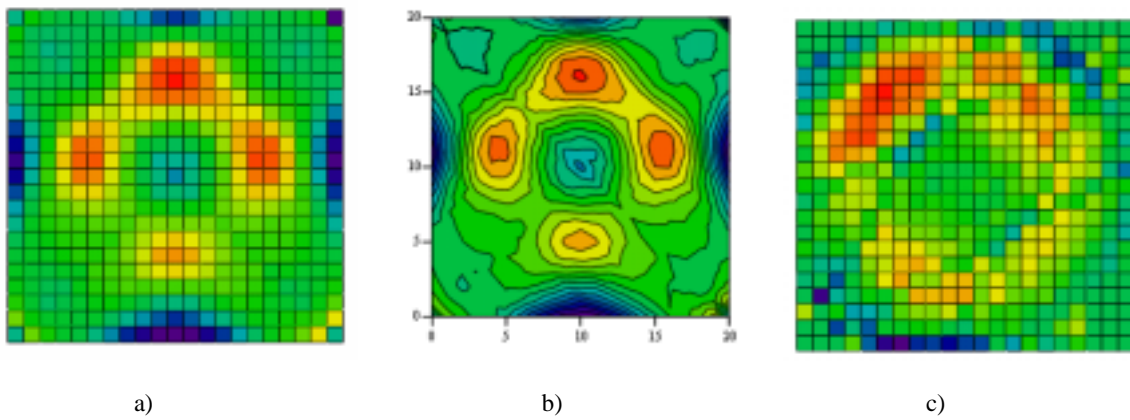


Figure 10. C₂ radical distribution tomographic reconstruction in (a) pixels four angular pictures (b) contour lines four angular pictures (c) C₂ radical distribution tomographic reconstruction in six angular pictures pixels.

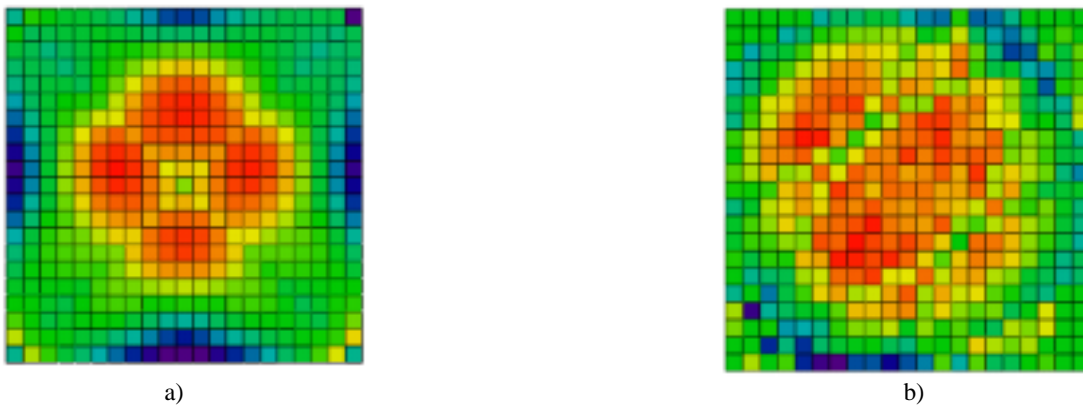


Figure 11. Soot radical distribution tomographic reconstruction pixels (a) four angular pictures (b) six angular pictures.

6. Conclusions

The Figures 10 and 11 show the reconstruction with different numbers of projections (photos). From these figures one can see that this flame is axially asymmetric with two concentric cones. The inner one is due to the first reaction zone, a premixed flame where the fuel is mixed with the oxygen.

In the second one, the more external cone, there are products and non burnt chemical substances from the first reaction that are burnt now, reacting with each others or with the atmospheric air, in the boundaries of the flame in a diffusive way.

The average images are justified by considering the flame a steady state dynamical flow. However, this is not true in the majority of the cases. This experiment is a first one in the test of a simple method involving the back projection and ART algorithms. One can observe that considerations of axial symmetry, Fig. 9, give rise to wrong conclusions.

Increasing number of projections (4 to 6) one can see a better definition in the contour of the flame although blurring the reconstructed image. This effect can be corrected by change the ART method considering the pixels areas instead of the ray sum length.

7. References

- Andersen, A. H., 1989, "Algebraic Reconstruction in CT from Limited Views", IEEE Transactions on Medical Imaging, Vol.8, pp. 50-55.
- Censor, Y., 1983 "Finite Series-Expansion Reconstruction Methods", Haifa Israel, proceedings of the IEEE, vol. 71, N°3 pp 409-419
- Herman, G. T., 1980 "Image reconstruction from projections", New York, Academic Press.
- Peterson, A. K. and , Oh, D. B., 2000, "Quantitative, High Sensitivity Diagnostics of Combustion Radicals Using Wavelength-Modulated UV Sources Sciences", Proceedings of the 38th Aerospace Sciences Meeting & Exhibit, USA, AIAA 2000 – 0777.
- Kaczmarz, M. S., 1937 "Angenäherte Auflösung von System linearer Gleichungen", Poland, Acad. Polon. Sci. Lett, pp355
- Kak, A. C., 1988 Computerized Tomographic Imaging, New York pp276-284.
- Peterson, A. K. and , Oh, D. B., 2000, "Quantitative, High Sensitivity Diagnostics of Combustion Radicals Using Wavelength-Modulated UV Sources Sciences", Proceedings of the 38th Aerospace Sciences Meeting & Exhibit, USA, AIAA 2000 – 0777.
- Radon, J., 1917, "Über die Bestimmung von Funktionen durch ihre Integralwerte längs gewisser Mannigfaltigkeiten", Vienna, Berichte der Sächsischen Akademie der Wissenschaft, pp. 262.
- VERÍSSIMO, A. S. *et al*, 2004, "Back Projection Tomography by the Simultaneous Equations Technique", XXVII Encontro Nacional de Física da Matéria Condensada, Poços de Caldas, Brazil, CD.
- VERÍSSIMO, A. S. *et a*, 2003, "Tomografia Computadorizada usando a Técnica Algébrica de Reconstrução com Iteração", Congresso Nacional de Matemática Aplicada Computacional, São José do Rio Preto, Brazil.
- Olson, W. T., *et al*, 1957, "Laminar Flame Propagation Tabela", NACCA Report 1300, JPL NASA, pp 323- 358.